

# Correction of Over- and Underexposed Images Using Multiple Lighting System for Exploration Robot in Dark Environments

Jonghoon Im<sup>1</sup>, Hiromitsu Fujii<sup>1</sup>, Atsushi Yamashita<sup>1</sup> and Hajime Asama<sup>1</sup>

**Abstract**— In this paper, we propose a method to correct the over- and underexposed regions in images. For the correction of over- and underexposed regions, multiple light sources are used to obtain several images whose over- and underexposed regions are in different positions. The image processing consists of four steps. Firstly, multiple images are captured by alternately turning on and off the illuminations set in different positions. Secondly, the luminance of the images acquired in step 1 is corrected. Thirdly, the over- and underexposed regions are extracted from the luminance-corrected images. Finally, the images are merged except for the over- and underexposed regions. The experiment results show that the over- and underexposed regions in the input images are recovered by our proposed method.

## I. INTRODUCTION

Nowadays, remote control robots are used in many dangerous places where people cannot enter. One such place is dark environments such as the Fukushima Daiichi nuclear power plant where the recent nuclear accident occurred in 2011. In order to investigate dark environments without the need for external lighting, as shown in Fig. 1, it is necessary to use robots that are equipped with their own lighting. However, when lights that are attached to the robot are used, it is difficult to illuminate targets sufficiently as compared to lights that are attached to the ceiling. In this case, the problem is that a portion of the image is unclear because of over- and underexposure. In such situations, the operator may have difficulty in controlling the robot.

In order to solve this problem, many methods have been proposed. One of the methods is High Dynamic Range imaging (HDRI) [1-2]. This technique obtains one image by combining a plurality of images with different exposure levels. For example, the bright areas are extracted from the images whose exposure values are decreased and the dark areas are extracted from the images whose exposure values are increased. The image is then clarified by combining the extracted areas.

Another method is to use image blocks [3]. This method partitions the image domain into uniform blocks and, for each block, selects the image that contains the most information within that block. The selected images are then blended together using monotonically decreasing blending functions that are centered at the blocks and have the sum of 1 everywhere in the image domain.

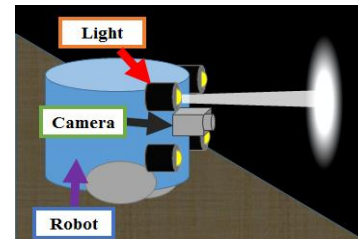


Fig. 1. Investigation using remote controlled robot with attached lighting.

These methods use adjustment of camera parameters such as ISO, shutter speed [4-6], and aperture, or specific devices such as beam splitters [7-9] for acquiring multi-exposed images. However, it is difficult to correct over- and underexposed areas using the previous methods in dark environments with no external lighting, such as that shown in Fig. 1. When the lighting is too strong, the light source is too close to the object, or the light is reflected from a material such as metal or glass, it is difficult to compensate for the irradiated regions using only adjustment of camera parameters. In such cases, it is necessary to change the lighting condition to correct for the irradiated regions.

One of the methods that utilize the changing of the light conditions is flash and no-flash imaging [10]. In this method, reflections and highlights from flash images are corrected by comparing the gradient information of the flash and no-flash images. However, if the environment has no external lighting, as is the case within the Fukushima Daiichi nuclear power plant, the no-flash image has no information about brightness and color. For this reason, this method has difficulty in correcting the over- and underexposed areas in environments with no external lighting.

Another method is the interactive digital photomontage [11]. In this method, the user begins with a set of multiple source images taken under different lighting conditions, and attempts to create a final composite image with attractive lighting. However, in this method, the user has to set each area manually for the composite. For this reason, this method is not appropriate as an over- and underexposure correction method in the exploration of dark environments where automatic processing is required.

To solve these problems, we propose a new method to correct the over- and underexposed regions in images using on/off control of multiple light sources for exploration in dark environments. In our previous research [12], automatic image processing was successful. However, the acquisition of multiple images was performed manually. Therefore, the image correction system could not be fully automated. In order

<sup>1</sup>J. Im, H. Fujii, A. Yamashita, and H. Asama are with the Department of Precision Engineering, Faculty of Engineering, The University of Tokyo, 7-3-1 Hongo, Bunkyo-ku, Tokyo 113-8656, Japan. (e-mail: {im, fujii, yamashita, asama}@robot.t.u-tokyo.ac.jp).

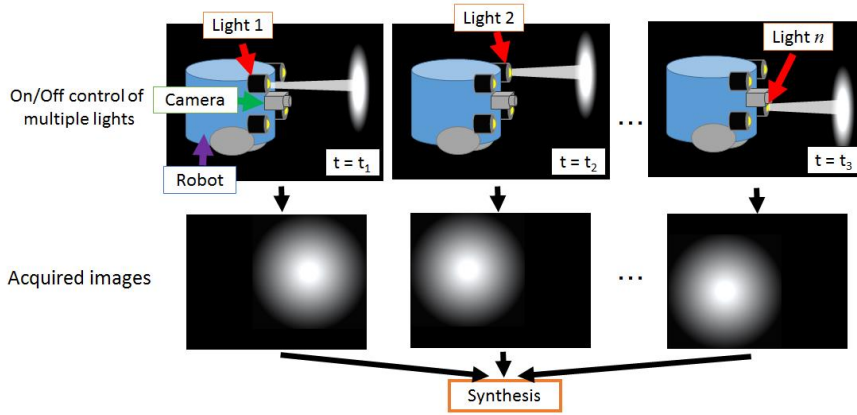


Fig. 2. Main concept of our proposed method for the correction of over- and underexposed regions using multiple images obtained by on/off control of multiple light sources.

to overcome this issue, we propose a new image correction method that automatically corrects over- and underexposed regions from image acquisition to image processing.

The rest of the paper is organized as follows. Section II describes the proposed method, and Section III depicts the experiment and its result. Finally, Section IV concludes the paper.

## II. PROPOSED METHOD

We propose a method for the compensation of over- and underexposed regions in an image by alternately turning on and off multiple light sources set in different positions. We assume the situation in which the operator is investigating a dark environment using a remote control robot, such as that shown in Fig. 1. Multiple light sources, such as headlights, are attached to the front of the robot, and each source can be turned on and off by the operator. Figure 2 shows the main concept of our correction method. When the over- or underexposure appears on the monitor that the operator is using, the operator is able to decide which light sources to turn on or off. Initially, only one light is switched on and others are switched off. The lights are then cycled through automatically, so that a single light at each position is turned on in succession. This process repeats until a stop command is issued by the operator. As a result of this process, multiple images whose over- and underexposed areas appear at different positions are acquired. By synthesizing properly exposed areas from each image, composite images with the desired exposure are acquired.

The schematic view of our proposed method is shown in Fig. 3. The image processing consists of four steps. Firstly, multiple images are acquired by alternately turning on and off multiple illuminators that are set in different positions. Secondly, the luminance of the input images is corrected. Thirdly, over- and underexposed regions in the luminance-corrected images are extracted. Finally, the images are merged except in the over- and underexposed regions. Each step is described in detail in this paper and prepared sample images are used to explain the process of our proposed method.

### A. Image Acquisition

In this process, multiple photographs with over- and underexposed areas in different locations are captured by changing the lighting condition. In this study, multiple images are acquired by alternately turning on and off each illuminator set in different positions. Figure 4 shows an example of synchronizing each camera frame with time interval for switching on and off of the lights when 2 lights are used. The process consists of 4 step. Firstly, light 1 is only switched on. Next, all of the lights are switched off. Then, light 2 is only switched on. Finally, all of the lights are switched off once again. The time interval between each process is set to be the same. The acquired images when each light is switched on are

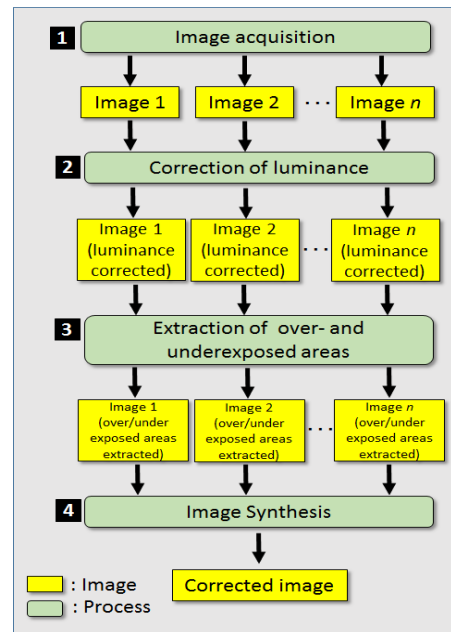


Fig. 3. Schematic view of our proposed method for the correction of over- and underexposure using multiple images obtained in a multiple lighting system.

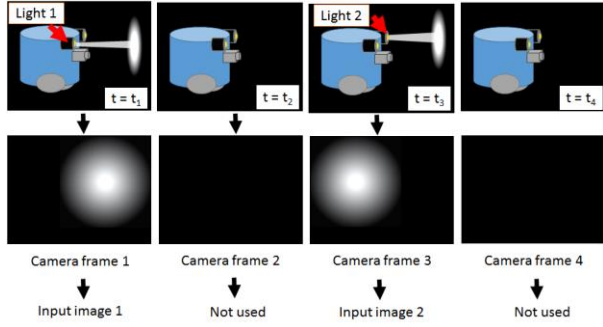


Fig. 4. Example of synchronizing each camera frame with time interval for switching on and off of the lights when 2 lights are used.

defined input images and used in image processing. However, the images obtained when all of lights are switched off not used in image processing. The object of switching off all of lights is to avoid afterglow which occurs between  $t = t_1$  and  $t = t_3$ . This process repeats and input images are continuously acquired.

The first acquired image is set to input image 1 ( $I_0^1$ ) and the next image is set to input image 2 ( $I_0^2$ ), and so on, until the final image is set to input image  $N$  ( $I_0^N$ ). Figure 4 shows sample images that were obtained in the image acquisition step. The over- and underexposed areas are shown on the left and right sides of the image in Fig. 5(a), respectively. Similarly, the over- and underexposed areas are shown on the right and left sides of the image in Fig. 5(b), respectively. In Fig. 5(c), the overexposed area is shown in the middle of the image and the underexposed area is shown at the edges of the image.

### B. Correction of Luminance

The brightness distribution of the input images is changed by the illumination condition. It can be confirmed by comparing Fig. 5 (a), (b), and (c) that different areas of exposure are acquired by changing the light condition. If the over- and underexposed areas in the input images are directly compensated by non-over- and non-underexposed areas in the other input images, the brightness between the compensated and non-compensated areas is different. In order to solve this problem, it is necessary to correct the brightness distribution of the acquired input images. As shown in Fig. 5(a), (b), and (c), the region around the center of the irradiated area is the brightest, and the luminance gradually decreases as the distance of each pixel from the center of the irradiated area becomes larger. In this step, we correct the luminance of the

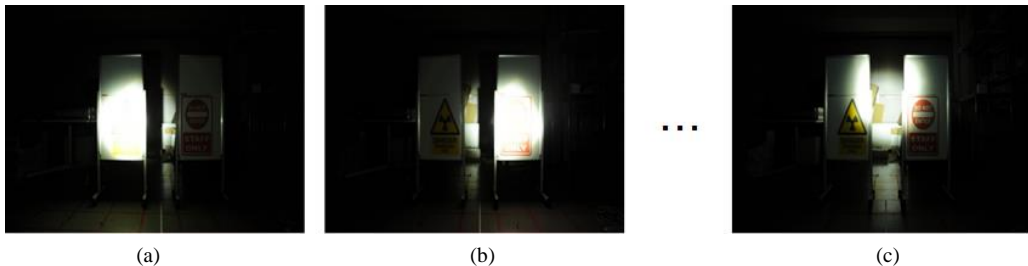


Fig. 5. Images obtained in the image acquisition step: (a) Input image 1  $I_0^1$  that is obtained at  $t = t_1$ , (b) input image 2  $I_0^2$  that is obtained at  $t = t_2$ , and (c) input image  $n$   $I_0^n$  that is obtained at  $t = t_n$ .

input images using the inverse-square law, which means that the brightness is inversely proportional to the square of the distance between the light source and the object. Therefore, if the brightness of each pixel and the square of the distance between the light source and the object are multiplied, the brightness of the input images becomes uniform. Equation (1) is used to correct the luminance of the images.

$$I_p^n(i, j) = \alpha \cdot I_0^n(i, j) \cdot d^2, \quad (1)$$

where  $n$  is the number of input images.  $I_0^n(i, j)$  is the luminance value of the input image at the coordinates  $(i, j)$ . The luminance value describes how bright a pixel is.  $I_p^n(i, j)$  is the obtained image as a result of the luminance correction process.  $\alpha$  is the correction factor that is set in advance by considering the environmental conditions.  $d$  is the distance between the light source and the object. In this step, we propose a new distance estimation method using only the input image. This method uses the principles of the straight propagation of light and the pinhole camera model, as shown in Fig. 6. Equations (2) and (3) describe each principle.

$$r = k \cdot l, \quad (2)$$

$$l = s \frac{f}{r'} r + c. \quad (3)$$

where  $l$  is depth and  $r$  is the vertical distance from the center of the irradiated area.  $r'$  is the vertical image distance from the center of the irradiated area.  $k$  is the proportional constant.  $s$  is the scale factor relating the pixels to the distance.  $f$  is the focal distance.  $c$  is the principal point that would ideally be located in the center of the image.  $p$  is the radius of the irradiated area; the irradiated area is defined as the area for which the luminance value of each pixel is over the threshold value  $\tau_c$ , which is set in advance by considering environmental conditions. In this step, we assume that the shape of the target object is a plane and it is in parallel to the image plane. To estimate  $d$ , it is necessary to estimate  $l$  and  $r$ .

$$d = \sqrt{l^2 + r^2}. \quad (4)$$

Equation (4) represents the relation between  $d$ ,  $l$ , and  $r$ . By substituting  $r$  of Eq. (2) into Eq. (3),  $l$  can be calculated from  $r'$ . If the value of  $r'$  changes, the value of  $l$  also changes. For this reason, it is necessary to fix a specific value of  $r'$ . In this study, we set the value of  $r'$  as  $p$  (Eq. (5)).

$$l = \frac{cp}{p - skf}. \quad (5)$$

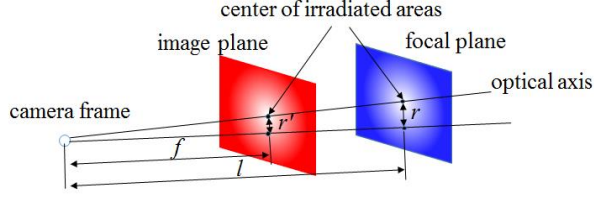


Fig. 6. Pinhole camera model.

Then,  $r$  can be estimated using the radius of the irradiated areas.

$$r = \frac{ckr'}{r' - skf}. \quad (6)$$

Next, by substituting  $l$  of Eq. (5) into Eq. (2),  $r$  can be calculated from  $r'$  (Eq. (6)).

$$d = \sqrt{\left(\frac{cp}{p - skf}\right)^2 + \left(\frac{ckr'}{r' - skf}\right)^2}, \quad (7)$$

$$r' = \sqrt{(i - XC)^2 + (j - YC)^2}. \quad (8)$$

Finally, Eq. (7) is acquired by substituting  $l$  of Eq. (5) and  $r$  of Eq. (6) into Eq. (4).  $r'$  can be calculated by Eq. (8), where  $(i, j)$  is the position of each pixel in the image, and  $(X_c, Y_c)$  is the position of the center of the irradiated areas in the image.

As a result of the luminance correction, the luminance increases gradually when the distance between the center of the irradiated area and each pixel becomes larger, as shown in Fig. 7 (a), (b), and (c). However, the over- and underexposed areas in the luminance-corrected images are not perfectly compensated by the correction of luminance.

### C. Extraction of Over and Under Exposed Areas

This process extracts the over- and underexposed areas in the luminance-corrected images in order to remove these areas. The method using two threshold values for luminance has been widely used in many related publications [13-15] to extract over- and underexposed areas. In this method, if the luminance value of the input image is greater than the threshold value, it is overexposed. If the luminance value of the input image is less than the threshold value, it is underexposed. However, there is a problem in that white or black colors are classified as over- or underexposed, respectively. In order to solve this problem, we use luminance and spatial information for the extraction of over- and underexposed areas. It is possible to estimate the

position of the over- and underexposed areas by considering the position of the irradiated areas in the image. Equation (9) is used for the extraction of over- and underexposed areas.

$$D^n(i, j) = \begin{cases} 0 & \text{if } I_p^n(i, j) > \tau_H \text{ AND } r < r_L \\ 0 & \text{if } I_p^n(i, j) < \tau_L \text{ AND } r > r_H \\ 1 & \text{otherwise} \end{cases} \quad (9)$$

where  $I_p^n(i, j)$  is the luminance value of the luminance-corrected image at coordinates  $(i, j)$ .  $\tau_H$  and  $\tau_L$  are the threshold values for the luminance information and range from 0 to 255.  $r$  is the distance between the center of the irradiated areas and each pixel in the image.  $r_H$  and  $r_L$  are threshold values for the spatial information and range from 0 to the maximum distance in the image (diagonal distance).  $\tau_H$ ,  $\tau_L$ ,  $r_H$ , and  $r_L$  are set in advance by considering the environmental conditions.  $D^n$  is the reference matrix for determining over- and underexposed areas, and is obtained as a result of the extraction of the over- and underexposed areas. This reference matrix is defined as a determination image. If the luminance value at the input image coordinates  $(i, j)$  is greater than  $\tau_H$  and if the spatial value of the input image coordinates  $(i, j)$  is less than  $r_L$ , it is determined to be overexposed and the pixel value is converted to 0. If the luminance value of the input image coordinates  $(i, j)$  is less than  $\tau_L$  and if the spatial value of the input image coordinates  $(i, j)$  is greater than  $r_H$ , it is determined to be underexposed and the pixel value is converted to 0. Otherwise, it is determined as non-over- or non-underexposed and the pixel value is converted to 1. As a result, the determination image  $D^n$  is acquired. The over- and underexposed areas are displayed in black and non-over- and non-underexposed areas are displayed in white in Fig. 8(a), (b), and (c). The areas displayed in black in the center of the images are overexposed areas that are caused by direct irradiation. The areas displayed in black on the edge of the images are underexposed areas that are caused by lack of light from the light source.

### D. Image Synthesis

In this step, the areas that are not over- and underexposed from the luminance-corrected images are synthesized. The determination image  $D^n$  obtained in Section II-C, shown in Fig. 8, is used. The rule of the synthesis is shown in Eq. (10).

$$I_f(i, j) = \frac{\sum_{n=1}^N D^n(i, j) I_p^n(i, j)}{\sum_{n=1}^N D^n(i, j)}. \quad (10)$$

The areas where  $D^n(i, j) = 0$  in the determination image  $D^n$ , which are shown as black in Fig. 8, are not used for synthesis. The areas where  $D^n(i, j) = 1$  in the determination image  $D^n$ ,

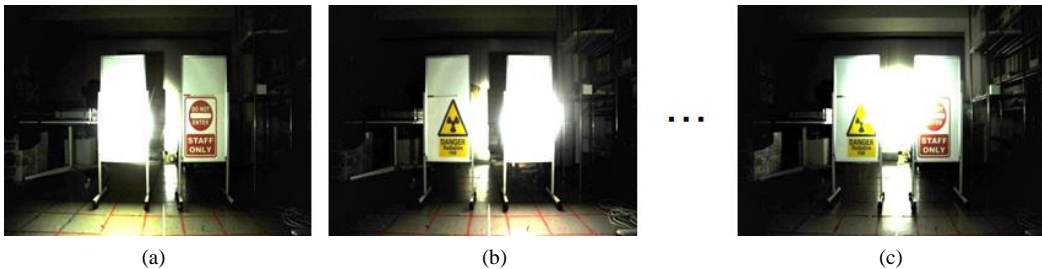


Fig. 7. Images obtained in luminance correction step : (a) Luminance-corrected image 1  $I_p^1$ , (b) Luminance-corrected image 2  $I_p^2$ , (c) Luminance-corrected image  $n$   $I_p^n$ .

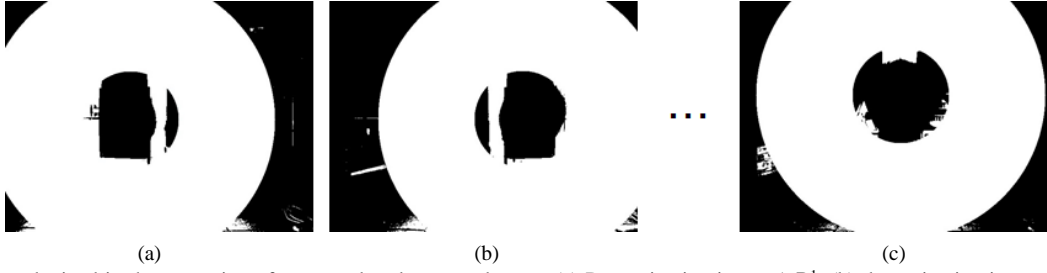


Fig. 8. Images obtained in the extraction of over- and underexposed areas: (a) Determination image 1  $D^1$ , (b) determination image 2  $D^2$ , and (c) determination image  $n D^n$ .

which are shown as white in Fig. 8, are used for synthesis. The areas that are not over- and underexposed are equally synthesized. As a result of this process, a corrected image  $I_f$  is obtained. Figure 9 shows the result of the synthesis. As a result of this process, the over- and underexposed areas from the input images, as shown in Fig. 5, are corrected. ‘DANGER Radiation risk’ on the left sign and ‘DO NOT ENTER, STAFF ONLY’ on the right sign became visible. The background of the input image also became clear.

### III. EXPERIMENT

#### A. Experimental Environment

Three lights were placed on the left, right, and top of the camera in order to acquire three images that showed over- and underexposure in different locations. Figure 10 shows the placement of the camera and the lights. The height of the camera was 800 mm from the floor. Light 1 was located in 300 mm left of the camera, and Light 2 was located 300 mm right of the camera. Light 3 was located 300 mm above the camera. All of the photographing conditions were fixed except the distance between the camera and the lights during the image acquisition process. The photographing conditions are depicted in Table 1. Finally, three images were acquired by alternately turning on and off each light. The experiment was performed in four different locations. All experiments were simulated on an Intel Core™ i5-2520M CPU 2.5 GHz PC with 8 GB RAM. In this experiment, we set  $\tau_C = 2.0 \times 10^2$ ,  $\tau_H = 1.2 \times 10^2$ ,  $\tau_L = 5.0$ ,  $r_L = 1.5 \times 10^2$ ,  $r_H = 2.3 \times 10^2$ ,  $\alpha = 1.2 \times 10^6$ ,  $k = 1.4 \times 10^{-1}$ ,  $s = 1.4 \times 10^2$  and  $c = 6.0 \times 10^2$ . The time interval between each camera frame and switching on and off of each lights are set to 1/60 s.

#### B. Experimental Result

The objective of the experiment is to verify whether the proposed method is valid in a variety of environments. Figures 11, 12, 13, and 14 describe the experimental results.



Fig. 9. Image obtained as a result of image synthesis step.

Figures 11 and 12 indicate plane environment, Fig. 13 and Fig. 14 represent no plane environment. The average computing time per frame was 0.21 s. Input image 1 in each figure was acquired when Light 2 was turned on, and input image 2 in each figure was acquired when Light 1 was turned on. Input image 3 in each figure was acquired when Light 3 was turned on. The corrected image in each figure represents the resulting image that was combined by our proposed method. In input image 1, the overexposure was shown on the left side of the image and the underexposure was shown on the right side of the image. On the other hand, the overexposure was shown on the right side and the underexposure was shown on the left side of input image 2. In input image 3, the overexposed areas were shown on the top center of the image and the underexposed areas were shown on the edges of the image. The over- and underexposed areas of the input images lost their color information and, consequently, it is difficult to identify the over- and underexposed areas. As a result of applying the proposed compensation algorithm to the input images taken in a variety of environments, the over- and underexposed areas in the input images became clear and it was possible to identify them in the output images.

However, if the over- or underexposed areas in one input image corresponded to those in the other input images, it was not successfully corrected. In order to solve this problem, it is necessary to acquire images that do not have the

TABLE 1. Photographing conditions.

<b>Camera</b>	NIKON D 700
<b>Definition</b>	640 × 480
<b>ISO</b>	400
<b>F-number</b>	f/8
<b>Shutter speed</b>	1/40 s
<b>Focal length</b>	24 mm
<b>Light</b>	GENTOS MF-1010G
<b>Luminance of light</b>	1,000 lm

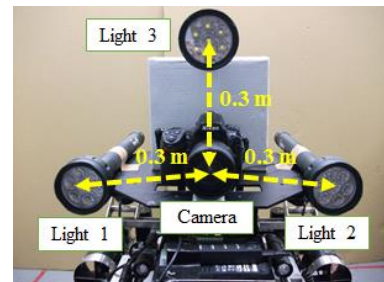


Fig. 10. Placement of camera and lights.



Fig. 11. Experimental result at location 1: (a) Input image 1, (b) input image 2, (c) input image 3, and the (d) corrected image.



Fig. 12. Experimental result at location 2: (a) Input image 1, (b) input image 2, (c) input image 3, and the (d) corrected image.

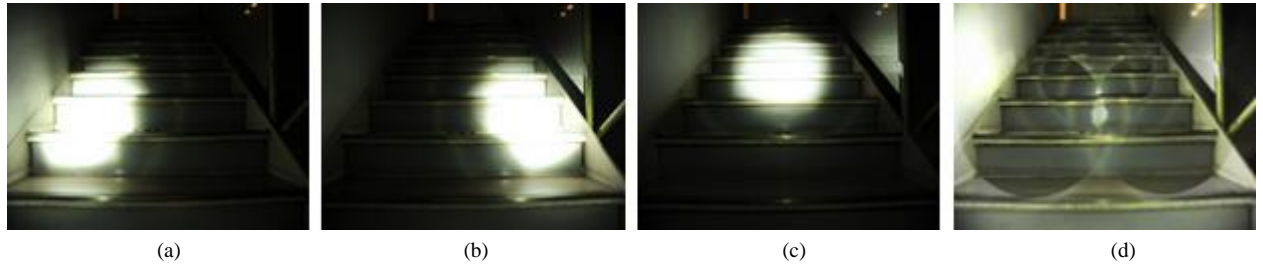


Fig. 13. Experimental result at location 3: (a) Input image 1, (b) input image 2, (c) input image 3, and the (d) corrected image.

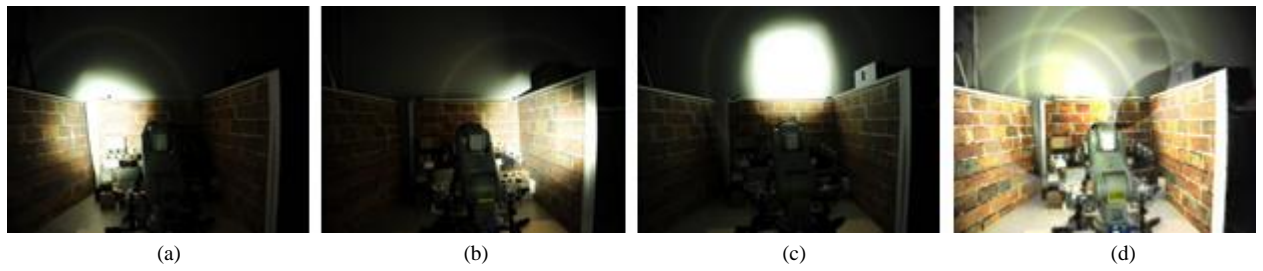


Fig. 14. Experimental result at location 4: (a) Input image 1, (b) input image 2, (c) input image 3, and the (d) corrected image.

over- and underexposed areas at the same locations in the input image and in the other images.

### C. Evaluation

We evaluated the proposed method with contrast compensation [16] and HDRI [2]. Entropy [17], which indicates the information value of the image, was used for the evaluation. If the image is overexposed or underexposed, the entropy of the image decreases. On the other hand, the entropy of the image increases if the brightness of the image is evenly distributed. The entropy was calculated using Eq. (11).

$$E = -\sum_{i=0}^L p_i \log(p_i), \quad (11)$$

where  $p_i$  is the probability that an arbitrary pixel in the image has intensity  $i$ .  $L$  is a gradation number and we set its value to 255.  $E$  is the entropy. Figure 15 and Table 2 show the entropy of the original image, the result of contrast compensation, the result of HDRI, and the result of our proposed method. The x-axis of the graph represents the images that are corrected by each method and the y-axis represents the entropy of each image. The blue column represents the entropy of the original image. The green column represents the entropy of the image that is corrected by contrast compensation. The orange column represents the entropy of the image that is corrected by HDRI. Finally, the red column represents the entropy of the image that is corrected by the proposed method. In all cases, the entropy of each image that was corrected by our proposed method is larger than that of the original image and of the images that

were corrected by contrast compensation and HDRI. This means that our proposed method is more effective than the contrast compensation and HDRI methods in dark environments. Next, we compared the computing time of each method. Table 3 shows the average computing time of each method. Contrast compensation takes 0.12 s for the image processing, while HDRI takes 0.61 s and the proposed method takes 0.21 s. Therefore, it can be seen that the average computing time of our proposed method is faster than that of HDRI and slower than that of contrast compensation.

#### IV. CONCLUSION

In this paper, we propose a new image correction method that automatically corrects over- and underexposed regions from image acquisition to image processing. We assumed a situation in which the operator investigates a dark environment using a remote control robot. Three lights are attached to the left, right, and top at the front of the robot, and each light can be turned on and off by the operator. Next, three images were acquired by alternately switching on and off the three lights. Finally, the over- and underexposed areas were compensated by the proposed method. The experimental results showed the effectiveness of our proposed method in a variety of environments.

For future work, we plan to apply our method to real situations, such as inside the Fukushima Daiichi nuclear power plant. Furthermore, it is necessary to control the brightness or adjust the angles of the lights in order to acquire more images in which the over- and underexposed areas will appear at different locations.

#### ACKNOWLEDGMENT

This work was funded by Tough Robotics Challenge, ImPACT Program of the Council for Science, Technology and Innovation (Cabinet Office, Government of Japan).

#### REFERENCES

- [1] S. Mann and R. W. Picard, "On being 'Undigital' with Digital Cameras : Extending Dynamic Range by Combining Differently Exposed Pictures," *Proceedings of the 48th Annual Conference of the Imaging Science and Technology*, pp. 442-448, 1995.
- [2] P. Debevec and J. Malik, "Recovering High Dynamic Range Radiance Maps from Photographs," *Proceedings of ACM SIGGRAPH 1997*, pp. 369-378, 1997.
- [3] A. A. Goshtasby, "Fusion of Multi-exposure Images," *Journal of Image and Vision Computing*, Vol. 23, No. 6, pp. 611-618, 2005.
- [4] D. C. H. Schleicher and B. G. Zagar, "High Dynamic Range Imaging by Varying Exposure Time, Gain and Aperture of a Video Camera," *2010 IEEE Instrumentation and Measurement Technology Conference*, pp. 486-491, 2010.

TABLE 2. Result of entropy comparison.

Method	Location1	Location2	Location3	Location4
Original image	2.52	3.29	3.35	3.18
Contrast compensation	3.00	3.48	3.35	3.59
HDRI	3.43	3.77	3.43	3.71
Proposed method	3.50	3.79	3.50	3.72

TABLE 3. Average computing time of each method.

Method	Time (s)
Contrast compensation	0.12
HDRI	0.61
Proposed method	0.21

- [5] Y. Piao and W. Xu, "Method of Auto Multi-Exposure for High Dynamic Range Imaging," *2010 International Conference on Computer, Mechatronics, Control and Electronic Engineering*, Vol. 6, pp. 93-97, 2010.
- [6] N. Barakat and T. E. Darcie, "Minimal Capture Sets for Multi-Exposure Enhanced-Dynamic-Range Image," *2006 IEEE International Symposium on Signal Processing and Information Technology*, pp. 524-529, 2006.
- [7] M. D. Tocci, C. Kiser, N. Tocci and P. sen, "A Versatile HDR Video Production System," *ACM Transactions on Graphics*, Vol. 30, No. 4, pp. 41, 2011.
- [8] M. Aggarwal and N. Ahuja, "Split Aperture Imaging for High Dynamic Range," In *Proceedings of IEEE International Conference on Computer Vision 2001*, pp. 10 – 17, 2001.
- [9] M. Aggarwal and N. Ahuja, "Split Aperture Imaging for High Dynamic Range," *International Journal of Computer Vision* 58, pp. 7–17, 2004.
- [10] A. Agrawal, R. Raskar, S. Nayar and Y. Li, "Removing Photography Artifacts Using Gradient Projection and Flash-Exposure Sampling," *ACM Transactions on Graphics*, Vol. 24, No. 3, pp. 828-835, 2005.
- [11] A. Agarwala, M. Dontcheva, M. Agarwala, S. Druckers, A. Colburn, D. Salesin and M. Cohen, "Interactive Digital Photomontage," *Proceedings of the 8th IEEE International Conference on Computer Vision*, pp. 10-17, 2001.
- [12] J. Im, H. Fujii, A. Yamashita and H. Asama, "Compensation of Over and Under Exposure Image Using Multiple Light Switching," *Proceedings of the 2014 IEEE/SICE International Symposium on System Integration (SII2014)*, pp.147-152, 2014.
- [13] W. Zhang and W. K. Cham, "Gradient-Directed Multi-Exposure Composition," *IEEE Transactions on Image Process*, Vol. 21, No. 4, pp. 2318–2323, 2012.
- [14] T. Jinno and M. Okuda, "Multiple Exposure Fusion for High Dynamic Range Image Acquisition," *IEEE Transactions on Image Process*, Vol. 21, No. 1, pp. 358–365, 2012.
- [15] O. Gallo, N. Gelfand, W. Chen, M. Tico, and Kari Pulli, "Artifact-Free High Dynamic Range Imaging," *Proceedings of IEEE International Conference on Computational Photography*, pp. 1–7, 2009.
- [16] E. Reinhard and K. Devlin, "Dynamic Range Reduction Inspired by Photo receptor Physiology," *IEEE Transactions on Visualization and Computer Graphics*, Vol. 11, No. 1, pp. 13-24, 2005.
- [17] C. E. Shannon, "A Mathematical Theory of Communication," *Bell System Technical Journal*, Vol. 27, No. 3, pp. 379-423, 1948.

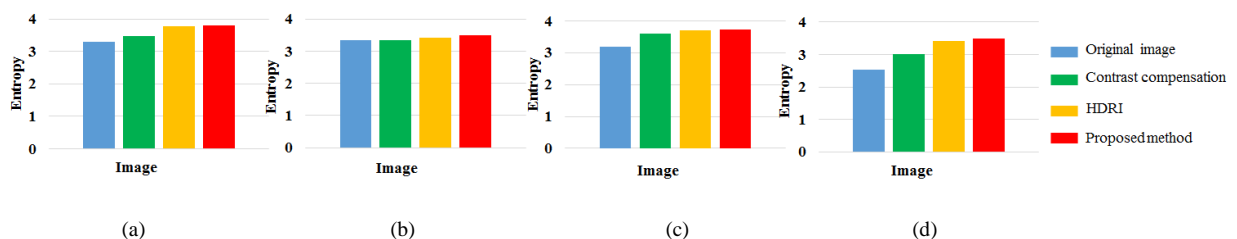


Fig. 15. Entropy of the original image (blue), the contrast compensation (green), the HDRI (orange), and our proposed method (red): (a) Location 1, (b) location 2. (c) location 3. and (d) location 4.